

Materials reliability for high-speed lithium niobate modulators

Hirotohi Nagata, Naoki Mitsugi, Junichiro Ichikawa,
and Junichiro Minowa

Optoelectronics Research Division, New Technology Research Laboratories,
Sumitomo Osaka Cement Co., Ltd.
585 Toyotomi-cho, Funabashi-shi, Chiba 274, Japan

ABSTRACT

As demand for lithium niobate optical modulators for use in high-speed optical communication systems has increased, their device performance and reliability have been vigorously improved, and some devices have found practical applications in systems. However, there are few reports, yet, about the quality and reliability of the lithium niobate material itself, although such information is necessary for improving further the device reliability and the fabrication yield. Here is presented data concerning material reliability for z-cut lithium niobate wafers commercially supplied in Japan. A variation is detected sometimes in the device performance such as dc-drift and optical insertion loss, and it seems to be caused mainly by an unpredictable fluctuation in the performance of individual wafers.

Keywords: lithium niobate, optical modulator, reliability, dc-drift

1. INTRODUCTION

Lithium niobate (LN) is a promising oxide material for fabrication of integrated optical circuits for high-speed communication systems, especially, the LN Mach-Zehnder intensity modulator and the LN polarization scrambler with 2.5 ~ 10 GHz optical bandwidth. These devices are tested for use in practical systems. Much reliability data for these packaged devices has been accumulated to indicate a satisfactory performance of more than 20-years-durability at ordinary operating conditions.^{1,2} Regarding the reliability of the packaged LN devices, the assembly technology, especially for fiber installation and for hermetically sealing the package, was an essential factor in achieving the high mechanical integrity.³ Only the dc-drift phenomenon, which was inevitably caused by the constituent materials, influenced the longterm stability of the modulators.⁴ Here, the problems depending on materials characteristics in the LN devices are presented from the view points on obtaining highly reliable devices and further improving device fabrication yield.

At first, the dc-drift phenomenon in z-cut LN Mach-Zehnder optical intensity modulators is presented, based on our recent investigation into devices in a commercial production range. Further, a possible dependency of the dc-drift behavior upon the applied dc bias voltage was found and is proposed here, although the origin of this phenomenon is not clarified, unfortunately, at this moment. Data such as magnitude of the dc-drift was also analyzed statistically to unveil the influence of the quality of the LN wafer on the dc-drift and consequently on the production yield of highly reliable LN modulators. This problem is presented in the second section with results for a similar analysis for other device performance. Finally, the influence of a continuous application of an electric field to the LN crystal, which seemed to involve partially the bias voltage dependency on the dc-drift, is presented, showing a domain inversion in the LN substrate as an example. Domain inversion was observed after dc-drift measurement with a constant dc bias voltage at temperatures elevated over 100 °C. This result was thought to be a meaningful phenomenon for investigating the mechanism of the failure of the LN devices, although under actual operation conditions, the devices were estimated experimentally to operate over 20 years without any deterioration in the performance.²

2. DC-DRIFT IN LN MODULATORS

When an electric field was applied to dielectric materials such as LiNbO₃ and SiO₂, the output performance from the materials changed chronologically, due to a relaxation of the movable ions, dipoles, *etc.* The dc-drift phenomenon in the optical output of the LN optical intensity modulators was also caused by the intrinsic nature of the dielectric materials, and could not be eliminated completely. A dc bias voltage was applied to the ac-operated modulators to adjust the state of the

optical output modulation, which increased generally as a result of the dc-drift. The magnitude of this dc bias needed to be suppressed below the limit of the dc driver throughout the operation for 20 ~ 25 years at 0 ~ 70 °C. In order to achieve reduced drift modulators, two device designs have been proposed and supplied commercially. The first method was ideal and aimed at dc bias-free modulators by adjusting the optical output modulation by the waveguide design and/or fabrication process.⁵⁻⁷ In such modulators, only a thermally induced drift appeared as the output fluctuation, although the magnitude of the thermal drift also changed drastically, depending on the device structure. The second more common method was applied to most commercial modulators, in which the magnitude of the dc-drift was reduced by altering the dielectric nature, *e.g.* permittivity, of the materials, especially the SiO₂ buffer layer.^{4, 8, 9} Here is presented the experimental data for the second type modulators, which consisted of a 0.5 mm thick z-cut LN substrate, an *x*-propagating Mach-Zehnder waveguide formed on the substrate by Ti-indiffusion, an approx. 1 μm thick SiO₂ layer by vacuum evaporation deposition, a thin Si layer, and Au coplanar electrodes.

2.1. Typical dc-drift behavior

Figure 1 shows the dc-drift at 100 °C measured for two different modulators cut from the closing position of the same LN wafer. The vertical axis denotes the drift voltage of the optical output peak position, due to the dc = 5 V application, from the unbiased state (ac = 1 kHz operated). As is seen, the drift proceeded negatively first, and then changed to an undesirable positive drift which consumed the initially applied dc bias. The negative drift was found to originate mainly in a retarding electrical response at the SiO₂ buffer layer, and its magnitude changed depending on the thickness and the chemical composition and structure of the buffer layer.^{4, 10} Recently, modulators consisting of a buffer layer chemically designed to have a large negative drift were reported to cancel the positive drift and successfully increase their stability.⁹

The positive drift was considered to have been caused mainly by the nature of the LN substrate because the magnitude of the drift was found to change depending on the amounts of proton impurity in the LN.^{11, 12} This drift voltage seemed to increase linearly against the logarithmic operation time, in other words, the drift rate decreased gradually in inverse proportion to the time. In the case of Fig. 1, the drift voltage at the 25th year at 50 °C (about 1580th hour at 100 °C) was extrapolated to be 1.2 V, assuming an activation energy $E_a = 1$ eV. Further, if the time dependency of the positive drift, $\Delta V(t)$, could be presented as $\Delta V(t) = A \ln(t) + B$, the intercept B and coefficient A were found to have a negative correlation as shown in Fig. 2, where the data for modulators with different buffer layer thicknesses, 0.8, 1.0 and 1.1 μm, were plotted. A reason for this relationship has not been clarified yet, but Fig. 2 shows the independency of the phenomenon upon the buffer layer thickness, supporting the consideration that the positive dc-drift was generated mainly at the LN substrate.

As mentioned above, the dc-drift consisted of a negative drift originating in the buffer layer and a positive drift originating in the LN substrate with the total drift voltage being more strongly influenced by the negative part due to the buffer layer. Because the magnitude of the negative drift was found to increase as the thickness of the layer increased, the modulators having the thicker SiO₂ layers were expected to be more durable. Actually, as is seen in Figs. 3 (a) for the lognormal cumulative distributions of drift-induced failures for the modulators of Fig. 2 and (b) for their failure rates, the modulators with thicker buffer layer were shown to work longer, even though the difference in their layer thicknesses was only 0.1 ~ 0.2 μm. In Fig. 3 (a), the vertical axis denotes the inverse normal of the cumulative distribution function (CDF) estimates for the lognormal failure distribution, and the -0.84 corresponds to 20 %, the 0 to 50 %, the 0.52 to 70 %, the 1.28 to 90 %, and the 1.64 to 95 %. Here, the failure point was determined to be the time when the drift voltage achieved 50 % of the applied dc bias voltage = 5 V at 100 °C, which was obtained by the extrapolation of measured results as done in Fig. 1. The same analysis had been attempted using a Weibull distribution, and the lognormal distribution was confirmed to match the dc-drift induced failures.

2.2. Screening test for dc-drift

Since the dc-drift was influenced by a fluctuation in the material's nature, the screening test was carried out for all modulators in order to detect failed modulators having a large drift due to uncontrollable material and process parameters. In this regard, an auto-bias controlled operation test at 80 °C for 100 h was performed for all LN intensity modulators, in which a dc voltage of 3.5 or 4.5 V was initially applied to the modulator and this dc voltage was adjusted to a frequency of 1 kHz so as to maintain the optical output modulation at the initial state. The magnitude of the initial dc bias voltage

corresponded to a halfwave voltage ($\lambda/2$) of the device. Note that the other method for Fig. 1 applied the constant dc bias voltage (= 5 V) throughout the test and was suitable for investigation of the drift mechanism.

Figure 4 shows the relationship between the auto-bias control measurement results at 80 °C for 100 h and the fixed bias measurement at 100 °C for 100 h. The auto-bias control measurement was carried out at first, and after aging the modulator in the unbiased state, the fixed bias measurement was performed for the same modulator. The vertical axes in Figs. 4 (a) and (b) denote the dc voltage including the initially applied bias of 3.5 V at the 100th hour and the voltage change from the 50th to 100th hours, respectively. Both the horizontal axes denote the drift ratio to the applied bias in percents at the 25th year at 50 °C, which was estimated from the fixed bias measurement results ($E_a = 1$ eV). Only in Fig. 4 (a), did a positive correlation appear, suggesting that the ultimate dc voltage achieved in the auto-bias controlled operation could be adopted as a criterion for screening out failed devices with large dc-drift. For instance, if the modulator being estimated to drift over 50 % during 25 years at 50 °C was determined to have failed, the criterion for the screening test would be set at 4.2 V.

2.3. Effect of dc bias voltage to dc-drift

The authors reported previously the phenomenon that the drift rate developed rapidly when an extraordinarily large dc bias was applied to the device as a result of auto-bias control.^{13,14} The experiment was done at 130 °C. The phenomenon was also observed in the fixed bias operation at the same temperature, and the dc-drift was abruptly accelerated after the 50-hour-operation with dc = 8 V application, although not with dc = 4 V. In addition to such an anomaly in the dc-drift which depended on the magnitude of the applied dc bias voltage, as shown in Fig. 5, it was observed that the sign of the applied voltage might possibly influence the dc-drift behavior, as well. This experiment was done at 130 °C using the auto-bias control method with initial bias voltages of ± 3.5 V. In the Figure, the thick and thin drift curves show the results for each pair of modulators which were cut from two different LN wafers, respectively. Each pair was cut from neighboring positions of their respective wafer, and they were expected to drift similarly as in the case of Fig. 1. The absolute values of the applied dc voltages for the modulators denoted by thick curves, increased in almost the same manner independent of the polarity of the initially applied dc bias. However, in the other modulators, the drift for the negatively biased modulator went over the limit of the bias control system (± 10 V) at the 400th hour unlike the positively biased one. The phenomenon needs to be further investigated.

3. ORIGIN OF THE VARIATIONS IN DEVICE PERFORMANCE

The quality of the LN wafer has been greatly improved by efforts to eliminate transition metal impurities to less than one ppm, to reduce crystal defects, *etc.*, and the 3 and 4 inch diameter wafers were commercially supplied from several manufacturers. However, the LN wafer quality and the following fabrication processes seemed not to be well established as yet. This section presents data showing that the variation in modulator performance depended on the LN wafer itself and the deposited buffer layers. Concerning the LN wafers, there was found a few lower-grade crystal boules (ingots) which provided wafers showing a large deterioration and variations in the fabricated device performance, even though they had passed a quality inspection such as a Curie temperature, chemical purity, *etc.* Furthermore, also from the ordinary crystal boules, some inferior wafers were found independent of the cut position in the boule. The results concluded that the fabrication lot of the devices could be defined as the individual LN wafer, not by the crystal boule nor by the region of the boule from which the wafers were cut. The data investigated here was for modulators fabricated using the z-cut wafers (optical grade) from two different Japanese companies. The Li/Nb chemical composition was slightly different between the two companies, judging from the Curie temperatures mentioned in their catalog sheets, 1133 and 1150 °C.

3.1. Optical insertion loss

The light propagating through the device was influenced by the quality of the waveguides, which depended in turn on the anomalous distribution of the Ti ions, the presence of microdomains, *etc.* Because the Ti-diffusion process was influenced by crystal defects and the Li/Nb ratio in the LN, in addition to the effects from the deposited metallic Ti thickness and annealing conditions, effects of the wafer lot was expected to appear in the optical insertion loss of the fabricated modulators. Figure 6 shows a distribution of the optical insertion losses for similarly fabricated Mach-Zehnder modulators, depending on the wafer lot. The optical insertion loss included a coupling loss between the waveguide, the installed thin film polarizer

and the fiber. The height of the bar in the Figure denotes the average for two modulators cut from almost the center of the same LN wafer. The marks A to O distinguish the difference in the LN crystal boules. As can be seen, there existed inferior boules, such as the J ~ O, and the modulators fabricated using the wafers from those boules showed rather large insertion losses. Note that the better boules also included a few inferior wafers, suggesting that the quality of the materials in the present LN needs to be further improved and homogenized. The dependency of the loss on the cut position of the wafer in the crystal boule was investigated for the boules A ~ I, and no characteristic distribution along the boule axis was found within the scattering of the data, as shown in Fig. 7. In Fig. 7, the direction for smaller numbers in the horizontal axis corresponds to the top of the boules where the seed had been attached for a crystal growth process.

As mentioned above, the device performance had been evaluated using two modulators from each supplied wafer, and the inferior wafers (and boules) were rejected from the production line for commercial modulators. Figure 8 reveals a coefficient of variation in the optical insertion loss for such commercial modulators made from the same wafer and also presents the results for 57 wafers from 10 different boules. From each wafer, more than ten modulators had been fabricated. The optical insertion loss, including the fiber coupling loss, was measured after a thermal-cure process of the adhesive material between the fibers and the device. The smaller coefficient of variation values indicated the narrower distribution of the obtained insertion loss and the higher fabrication yield with regard to a certain wafer. The distribution for the wafers in Fig. 8 was within an allowable range for the present device specification and did not increase significantly the number of rejected modulators. However, the reason for the existence of the extraordinarily wide (or narrow) distribution needs to be investigated. In this regard, we analyzed the data of Fig. 8 but unfortunately could not find any reason at this moment. For instance, the coefficients of variation values in Fig. 8 were replotted as a function of the wafer cut position in the crystal boule in Figs. 9 (a) for the boules from manufacturer A and (b) for manufacturer B. The marks in the Figures denote a difference in the boule and largely scattered without feature. Also, concerning the loss distribution on each individual wafer, no characteristic curves could be observed, as shown in Fig. 10. Figure 10 reveals the distribution of optical insertion losses normalized by the average for the modulators from the same wafer, which had been cut from the 3rd boule from the right side of Fig. 8.

At this moment, it can be said, at least, that the crystal and/or chemical quality of the present LN materials was not yet perfect regarding to inter- and intra-crystal boules. Some wafers produced LN modulators successfully having homogeneous performance and others did not, even though those wafers had been cut from the same boule. In other words, device manufacturers need to screen LN wafers based on the individual wafer lot rather than the boule lot.

3.2. Dc-drift

Because the dc-drift was complicated with both the LN substrate and SiO₂ layer, we could hardly determine the origin for the variations in the dc-drift, whether from the wafer or buffer layer. Table I shows the results of the dc-drift screening for the hermetically sealed modulators measured by the auto-bias control method at 80 °C for 100 h. The average, standard deviation (σ_{n-1}) and coefficient of variation for the applied dc voltages, including the initially 3.5 V bias, are listed for the wafers producing more than 10 modulators. The difference in the crystal boule, wafer, wafer manufacturer, SiO₂ thickness and its fabrication batch are also listed. Here, we attempt to classify the coefficient of variations to three grades, at the ~0.05, ~0.1 and over ~0.15, which are differently hatched in the Table. However, the main origin for the variation was not clearly seen, although the SiO₂ fabrication batch seemed to provide some influence on the magnitude of the variation. On the other hand, a correlation between the coefficients of variations for the optical insertion losses from Fig. 8 and for the dc-drifts from Table I was investigated as shown in Fig. 11, also revealing a weak positive correlation. The presence of impurities and crystal defects in the wafer might induce a larger scattering in the magnitude of both the optical insertion loss and the dc-drift.

Concerning the distribution of the drift magnitude on the wafer, a variation, possibly due to the unevenness in the SiO₂ buffer layer, was observed. Figures 12 (a) and (b) show the distribution of the applied dc voltages for the modulators having the 0.8 μm thick and 1 μm thick SiO₂ layers, respectively, which were normalized by the averages for the corresponding wafers (see Table 1). The horizontal axis of the Figures denote the chip position numbered along the y-axis of the wafer. The Figures include results for seven wafers in (a) and thirteen wafers in (b). Although there was some scattering data, the normalized applied dc voltage increased for the modulators cut at a position more apart from the center of the wafer. Since the dc-drift tended to be larger for the modulators with thinner SiO₂ layers, as described in Section 2,

these results suggested that the SiO₂ layer had been formed as thinner and/or less dense at the edge region of the wafer. In the SiO₂ deposition process for these wafers, the wafers were set on a revolving holder in the evaporation chamber as the manner for arranging the μ -axis of the wafer parallel to the diameter of the holder. In such an arrangement, there was the possibility that parameters in the SiO₂ deposition, such as a speed of incident particles and the deposited thickness, varied along the wafer μ -axis.

Table 1 Results of the dc-drift screening tests for the commercial Mach-Zehnder modulators fabricated using various z-cut LN wafers and SiO₂ buffer layer thicknesses.

Boule No.	Wafer No.	Manuf.	SiO ₂ thickness [μ m]	SiO ₂ fab.batch	Applied dc voltage at the 100th hour at 80°C (auto-bias control with the initial bias voltage =3.5V)				
					Average [V]	σ_{n-1} [V]	Coefficient of Var. [-]	Sample No.	
#30	#7	A	1	a	4.78	0.46	0.096	36	
	#9				3.48	0.40	0.115	12	
	#10				3.92	0.34	0.087	35	
	#11		0.8	b	4.00	0.40	0.100	21	
	#12				3.78	0.31	0.082	29	
#31	#4	1	c	3.74	0.51	0.136	30		
	#5			3.13	0.31	0.099	26		
	#6			2.95	0.23	0.078	30		
	#23	1	d	3.89	0.38	0.098	28		
	#25			3.72	0.17	0.046	25		
	#31	0.8	e	3.58	0.56	0.156	21		
	#34			4.25	0.49	0.115	24		
	#37	1	f	3.73	0.47	0.126	22		
#44	#21	1	g	4.03	0.54	0.134	27		
	#33			1.3	h	3.61	0.25	0.069	13
	#35			1	i	3.58	0.52	0.145	35
#53	#24	B	1	j	3.90	0.58	0.149	29	
	#33				4.48	0.61	0.136	11	
#58	#26	1.3	k	3.57	0.93	0.261	14		
	#27			3.40	1.19	0.350	16		
#62	#49	0.8	l	3.09	0.17	0.055	16		
	#56			3.19	0.22	0.069	17		
	#57			3.17	0.12	0.038	15		

3.3. Optical bandwidth

The optical bandwidth was expected to be greatly influenced by the dielectric nature of the SiO₂ layer. Table 2 is a list of the optical bandwidth measured for the commercial modulators, showing slight dependency on the SiO₂ fabrication batch. However, the correlation between the coefficient of variations for the optical bandwidth and for the dc-drift was unclear, compared with that between the optical insertion loss and the dc-drift in Fig. 11. This was thought to be a consistent result, because the variations in both the dc-drift and optical loss were caused by the quality fluctuation in the LN wafer, while the bandwidth was influenced mainly by the SiO₂. Figures 13 (a) and (b) reveal a distribution of the normalized optical bandwidths against the chip position in the wafers for the modulators with 0.8 μ m and 1 μ m thick SiO₂ layers, respectively. At the edge region on the wafer, the bandwidth became narrower because of the smaller SiO₂ thickness, being consistent with the result for the dc-drift of Fig. 12.

Table 2 Results of the optical bandwidth measurements for the commercial Mach-Zehnder modulators fabricated using various z-cut LN wafers and SiO₂ buffer layer thicknesses.

Boule No.	Wafer No.	Manuf.	SiO ₂ thickness [μ m]	SiO ₂ fab.batch	Optical bandwidth (3 dB down)					
					Average [GHz]	σ_{n-1} [GHz]	Coefficient of Var. [-]	Sample No.		
#30	#7	A	1	a	8.96	0.82	0.092	36		
	#10				9.28	0.55	0.059	35		
	#11		0.8	b	5.85	0.47	0.080	21		
	#12				5.77	0.43	0.074	29		
#31	#4	1	c	6.97	0.40	0.057	30			
	#5			9.28	0.66	0.071	26			
	#6			9.34	0.92	0.099	30			
	#23	1	d	7.47	0.98	0.131	28			
	#25			7.75	1.31	0.169	25			
	#31	0.8	e	6.13	0.33	0.054	21			
	#34			5.35	0.37	0.069	24			
	#37	1	f	6.64	0.17	0.026	22			
	#44	#21	1	g	9.23	0.37	0.040	27		
#35		1			i	8.94	0.61	0.068	35	
#53	#24	B	1.3	k	8.65	0.43	0.050	29		
#58	#27				11.42	2.56	0.224	14		
#62	#49				0.8	l	5.50	0.20	0.036	16
	#56						5.48	0.28	0.051	17
	#57	5.50	0.33	0.060			15			

4. POSSIBLE FATIGUE OF LN DUE TO APPLIED FIELD

At last, an effect of the applied dc bias voltage to the LN was investigated, because the possible bias voltage dependency was observed in the dc-drift at a high temperature, 130 °C, as described in the Section 2 . In the present modulators, because the dc bias voltage was applied almost parallel to the z-axis of the LN crystal, which was the polarization axis, the possibility of an occurrence of 180 °C domain inversion in the LN waveguides was predicted. Here, the possibility of this prediction at a lower temperature, 80 °C, was investigated.

The experiments were carried out using the common z-cut Mach-Zehnder modulator chips, which were composed of a 1 μ m thick SiO₂ layer, a thin Si layer, and Au coplanar electrodes with 25 μ m gaps between the hot and ground electrodes. In order to obtain whether the dc bias application induced the domain inversion, the Au electrodes were cut completely at the middle of the chip and the bias was applied to one of the divided hot electrodes . Two samples were prepared; sample 1 showed 205 k Ω for electrical resistance between the hot and ground (R_{h-g}) at room temperature, and sample 2 showed $R_{h-g} = 700 \Omega$. The dc bias voltages of 10 and 15 V were continuously applied to samples 1 and 2, respectively, at 80 °C for 100 h. Then, the samples were chemically etched by a 1 : 5 mixture of HF : HNO₃ for an observation of inverted domain.

Figure 14 shows optical micrographs of surfaces for sample 1 after the chemical etching: (a) for the unbiased waveguides and (b) for the biased waveguides. The bright area corresponds to the intrinsic -z LN surface, and the black spots (and area) indicate the microdomains with +z polarity. The larger spot-like micro-domains in the waveguides of Fig. 14 (a) were caused by the Ti-indiffusion process. In the biased waveguides, Fig. 14 (b), the micro-domains were concentrated in the region under the electrodes, indicating that the domain inversion occurred due to the large dc bias application, even at 80 °C. The 10 V dc bias for sample 1 was estimated to be on the order of 10⁵ V/m from the gap between the hot and ground electrodes. The micro-domain were also observed in sample 2, but the amounts were smaller than in sample 1 although the

applied dc bias was larger. As a reason for this inconsistent result, we considered the influence of the leak current magnitude on domain inversion at this moment, which was estimated to be two times larger in sample I having the lower R_{h-g} value. The mechanism of the domain inversion due to high dc bias application at such lower temperatures is to be clarified, and recently Prof. G. Rosenman of Tel Aviv Univ. proposed to us that the phenomenon was probably concerned with redistribution of the constitutions in the LN.¹⁵

Note that in the functional long-term aging test for twelve z-cut 10 Gb/s type modulators at 85 °C for 5000 h, the applied dc voltage by the auto-bias control never exceeded the 10 V and no deterioration was detected in the other device performance after the test. Further, the effect of a continuous ac = ±15 V application was investigated for six z-cut optical polarization scramblers at 90 °C for 1000 h, also leading to no degradation in their performance.

5. CONCLUSION

The quality and reliability of the LN crystals and wafers were evaluated from viewpoints of the reproducibility of the LN modulator devices with resultant high performance. In our experience for the device fabrication, we concluded that the LN materials were not well enough established yet as to homogeneity of their performance throughout the grown crystal boules for commercial wafers. The screening of the devices based on the individual wafers, at least, was necessary to reject the inferior wafers from the production line for commercial modulators. Furthermore, the nature of the LN materials needs to be further studied for unveiling the key factors to improve the device reliability. The possibility of domain inversion due to the dc bias application was found at temperatures within a range for the device operation. In this regard, for instance, problems like ferroelectric fatigue, which was commonly observed in perovskite materials during their ac operation as increasing leak currents and decreasing polarization,¹⁶ also needs to be investigated for the LN crystal and other device constituent materials.

6. ACKNOWLEDGMENTS

Authors thank gratefully staff members of the LN-group of the optoelectronics division for their efforts in development and fabrication of LN modulator devices and especially Mr. Kiuchi for his help in using the database system for the analyses.

7. REFERENCES

1. H. Nagata and N. Mitsugi, Mechanical reliability of LiNbO₃ optical modulators hermetically sealed in stainless steel packages, *Opt. Fiber Technol.*, vol. **2**, 216-224, 1996.
2. H. Nagata, N. Mitsugi, K. Kiuchi, and J. Minowa, Lifetime estimation for hermetically packaged 10 Gb/sec LiNbO₃ optical modulators, *Eng. & Lab. Notes, Opt. & Phot. News*, vol. **7** (11), 1996.
3. H. Nagata, N. Mitsugi, M. Shiroishi, T. Saito, T. Tateyama, and S. Murata, Elimination of optical fiber breaks in stainless steel packages for LiNbO₃ optical modulator devices, *Opt. Fiber Technol.*, vol. **2**, 98-105, 1996.
4. H. Nagata and J. Ichikawa, Progress and problems in reliability of Ti:LiNbO₃ optical intensity modulators, *Opt. Eng.*, vol. **34** (11), 3284-3293, 1995.
5. A. S. Greenblatt, C. H. Bulmer, R. P. Moeller, and W. K. Burns, Thermal stability of bias point of packaged linear modulators in lithium niobate, *J. Lightwave Technol.*, vol. **13** (12), 2314-2319, 1995.
6. F. J. Leonberger, D. E. Bossi, R. W. Ade, and D. K. Lewis, Manufacturing and applications of integrated optical circuits, *Proc. 8th Ann. Meet. IEEE Lasers and Electr. Opt. Soc.*, Part 2, 257-258, 1995.
7. P. G. Suchoski, Jr. and G. R. Boivin, Reliability and accelerated aging of LiNbO₃ integrated optic fiber gyro circuits, *SPIE*, vol. **1795**, 38-47, 1992.
8. Y. Nakabayashi, M. Kitamura, and T. Sawano, Dc-drift free-polarization independent Ti:LiNbO₃ 8x8 optical matrix switch, *Proc. ECOCI96, Oslo*, Part **4**, 157-160, 1996.
9. M. Seino, T. Nakazawa, S. Taniguchi, and M. Doi, Improvement of dc-drift characteristics in Ti:LiNbO₃ modulator, *Technol. Rep. IEICE*, vol. OCS95-66, **55-60**, 1995.
10. H. Nagata, H. Takahashi, H. Takai, and T. Kougo, Impurity evaluation of SiO₂ films formed on LiNbO₃ substrates, *Jpn. J. Appl. Phys.*, vol. **34** Part I (2A), 606-609, 1995.

11. H. Nagata, J. Ichikawa, M. Kobayashi, J. Hidaka, H. Honda, K. Kiuchi, and T. Sugamata, "Possibility of dc drift reduction of Ti:LiNbO₃ modulators via dry O₂ annealing process," *Appl. Phys. Lett.*, vol. **64** (10), I 180-1182, 1994.
12. H. Nagata, J. Ichikawa, N. Mitsugi, T. Sakamoto, T. Shinrild, H. Honda, and M. Kobayashi, "Improved long-term dc drift in OH-reduced lithium niobate optical intensity modulators," *Eng. & Lab. Notes, Opt. & Phot. News*, vol. **7** (5), 1996.
13. H. Nagata, N. Mitsugi, T. Sakamoto, K. Kiuchi, and J. Ichikawa, "Applied-voltage induced fatigue of lithium niobate waveguide," *Appl. Phys. Lett.*, vol. **68** (3), 301-303, 1996.
14. N. Mitsugi and H. Nagata, "Hysteresis in dc bias drift of LiNbO₃ optical modulators," *Eng. & Lab. Notes, Opt. & Phot. News*, vol. **7** (8), 1996.
15. G. Rosenman, V. D. Kugel, and D. Shur, "Diffusion-induced domain inversion in ferroelectrics," *Ferroelectrics*, vol. **172**, 7-18, 1995.
16. C. A. Araujo, J. D. Cuchiari, L. D. McMillan, M. C. Scott, and J. F. Scott, "Fatigue-free ferroelectric capacitors with platinum electrodes," *Nature*, vol. **374** (13), 627-629, 1995.

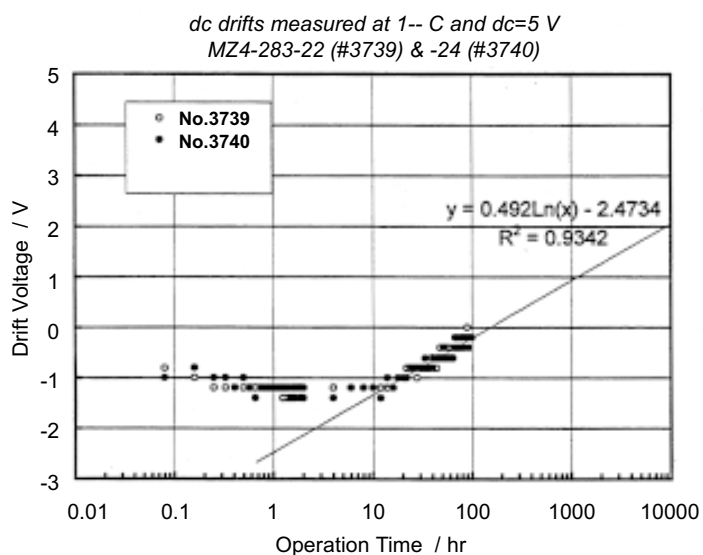


Fig. 1 Dc-drift measured at 100 °C by a fixed dc = 5 V bias voltage method.

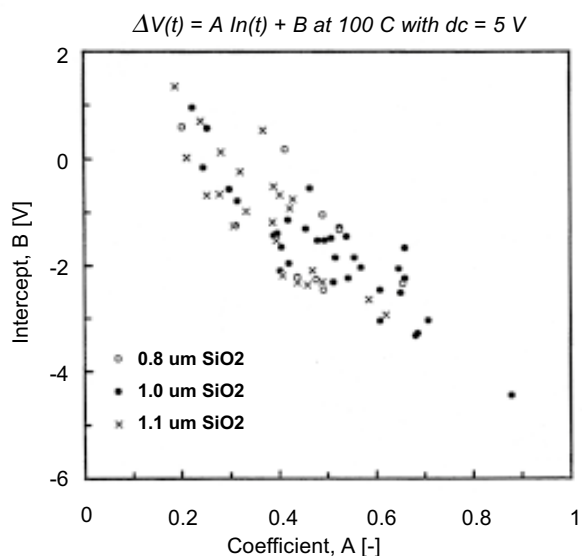


Fig. 2 Correlation between the intercept B and coefficient A in the equation, $A \ln(t) + B$, for the dc-drift as a function of time, t.

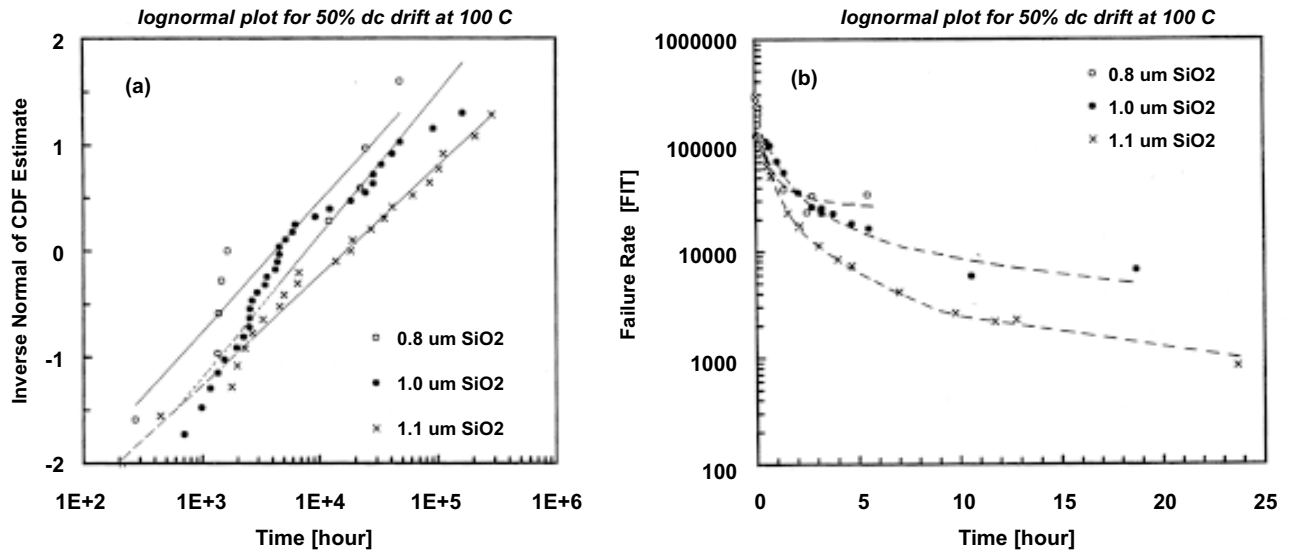


Fig. 3 Lognormal distribution plots for device failures due to the dc-drift. (a) for a cumulative failure distribution and (b) for a failure rate.

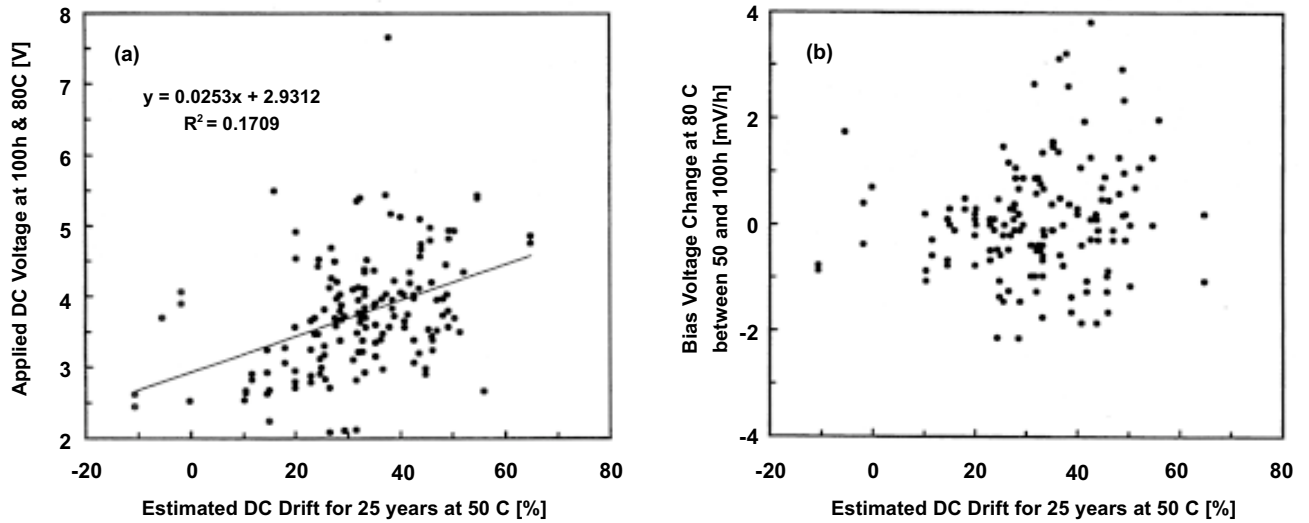


Fig. 4 Correlation between results of the dc-drift measurements by an auto-bias control method (vertical axis) and by a fixed dc bias method (horizontal axis). The ultimate applied dc bias voltage at the 100th hour in the auto-bias control method is plotted in the vertical axis in (a), and the bias voltage change from the 50th to 100th hours is plotted in (b).

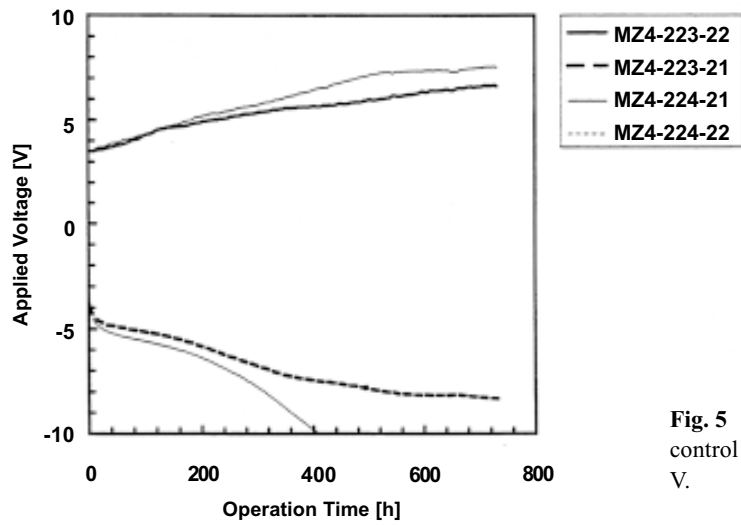


Fig. 5 Dc-drifts measured at 130 °C by the auto-bias control method with initially applied dc voltages of ± 3.5 V.

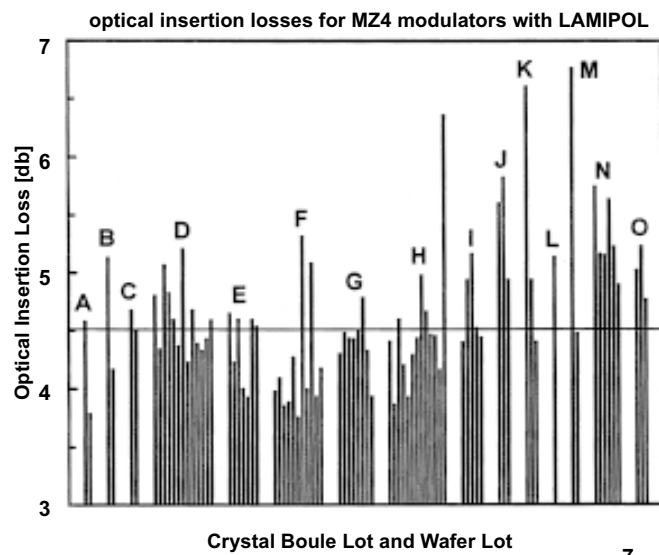
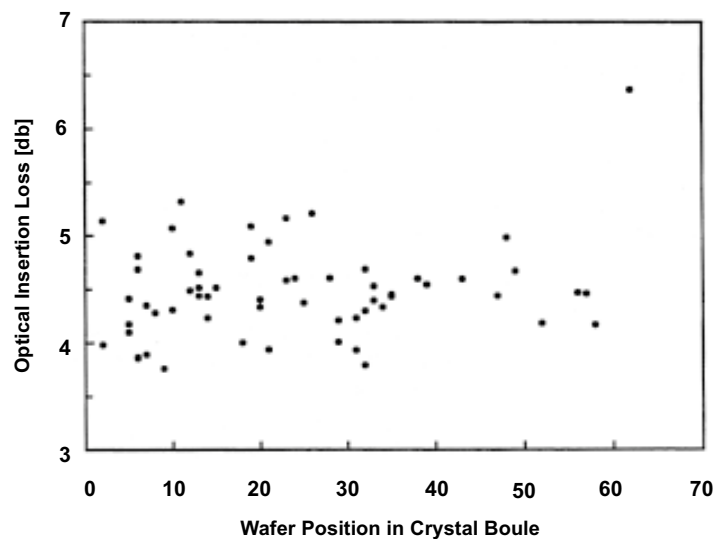


Fig. 6 Dependence of optical insertion losses of the modulators LN crystal boule and wafer.

Fig. 7 Dependence of optical insertion losses of the modulators upon wafer cut position from the boule.



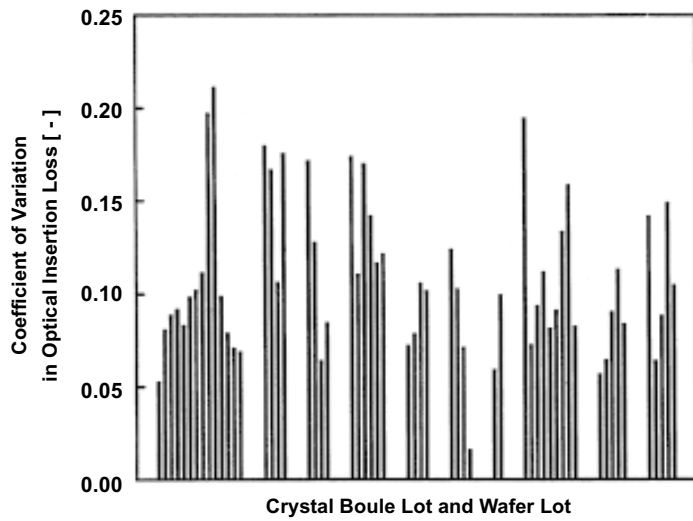


Fig. 8 Dependence of coefficient of variation of the optical insertion loss upon LN boule and wafer.

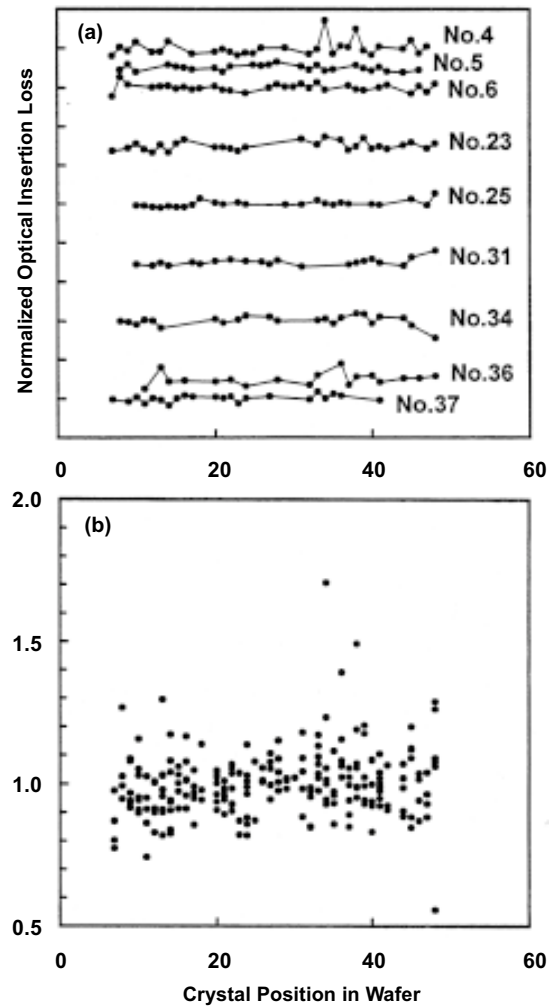
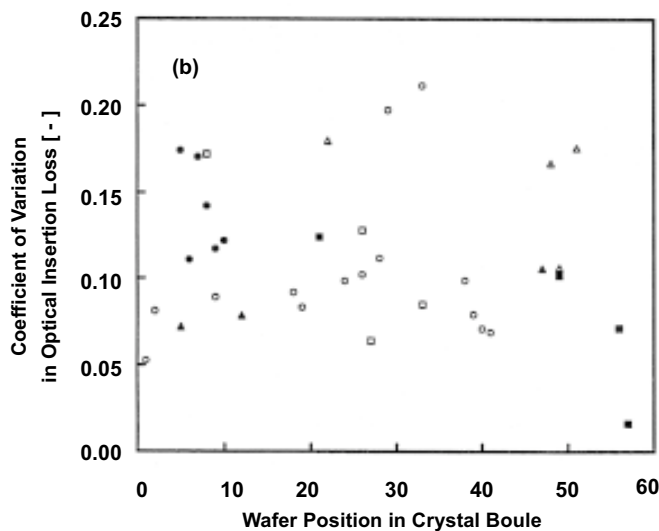
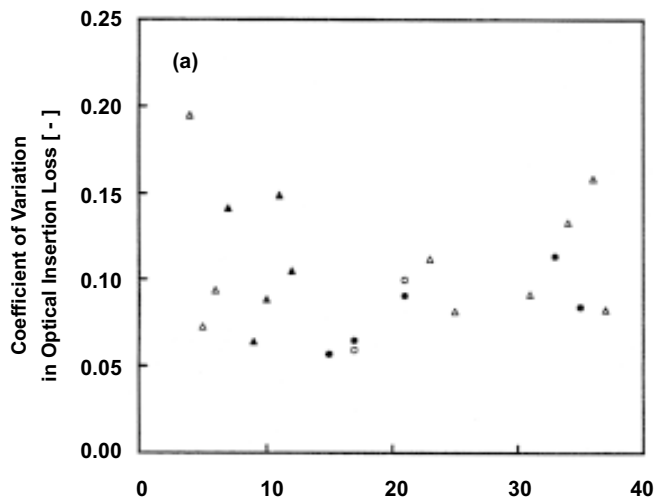


Fig. 10 Dependence of normalized optical insertion losses upon the wafer position from which device chips were cut. Numbers in (b) denote cut position of the wafer from the LN boule.

Fig. 9 Dependence of coefficient of variation of the optical insertion loss upon wafer cut position from the boule. (a) for the wafers supplied from the manufacturer ěÁÍ and (b) for the manufacturer ěBÍ .

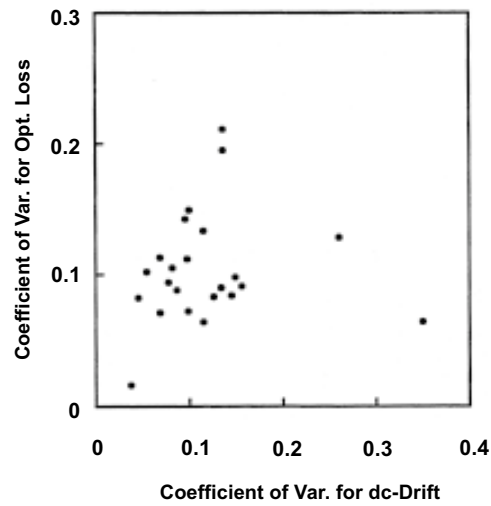


Fig. 11 Correlation between coefficient of variations for optical insertion loss and for dc-drift.

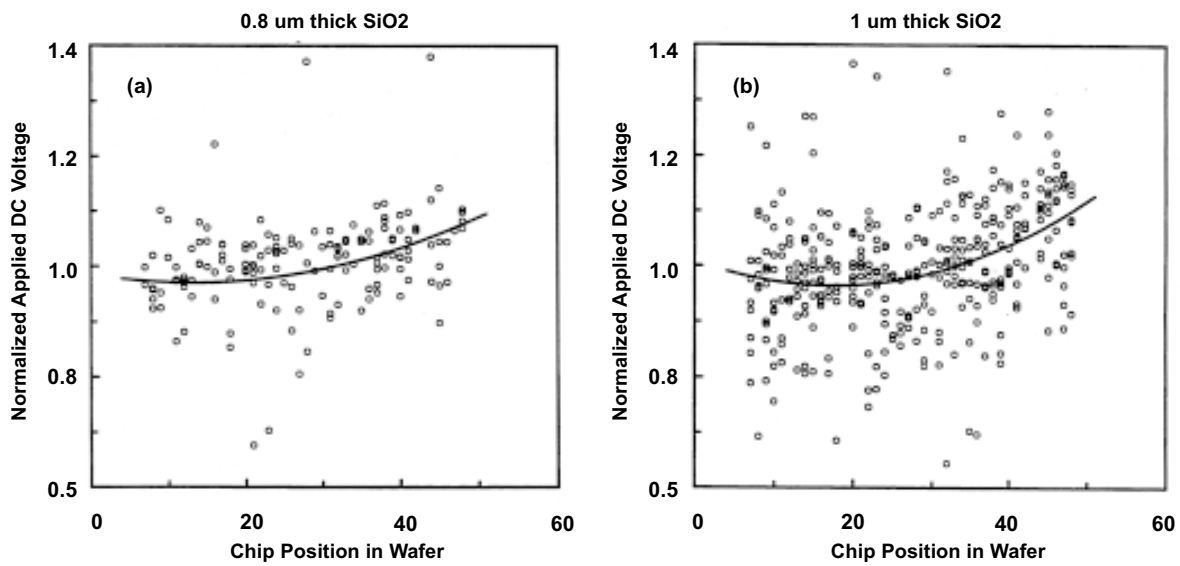


Fig. 12 Dependence of normalized applied dc bias voltage in the auto-bias controlled operation upon chip position in the wafer. (a) for the modulators with 0.8 μm thick SiO_2 buffer layer and (b) for the modulators with 1 μm thick SiO_2 .

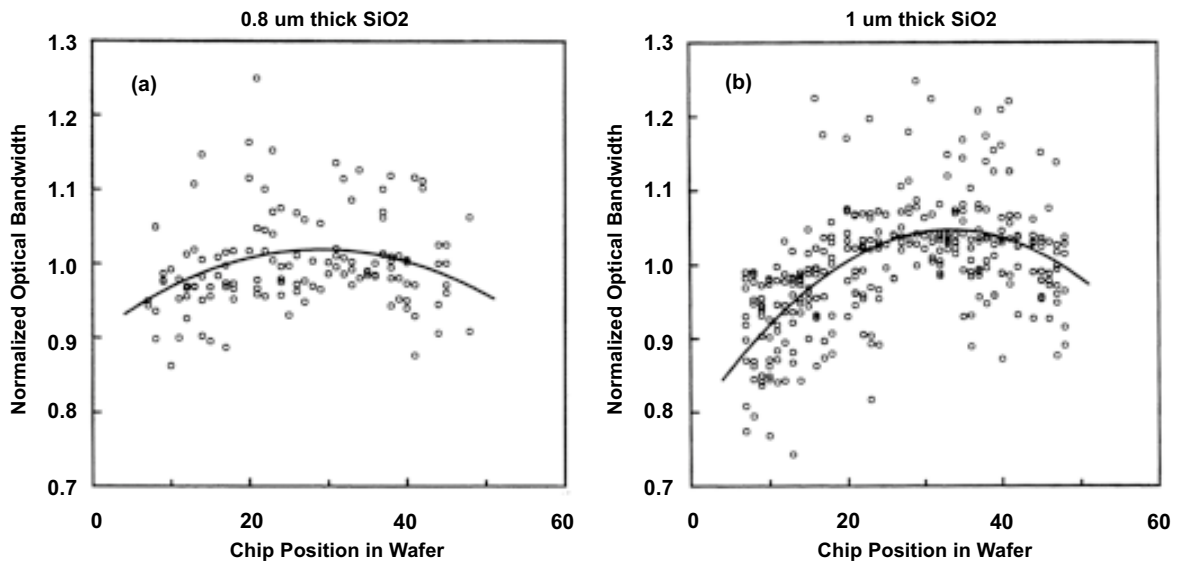


Fig. 13 Dependence of normalized optical bandwidth upon chip position in the wafer. (a) for the modulators with 0.8 μm thick SiO₂ buffer layer and (b) for the modulators with 1 μm thick SiO₂.

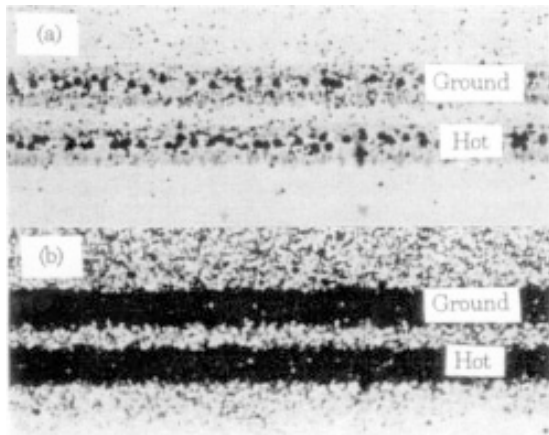


Fig. 14 Etched LN surface (a) without dc bias and (b) with dc = 10 V bias at 80 °C for 100 h.